STRUCTURAL STUDIES IN ZnO NANOPARTICLES AND Li_2O DOPED POLYPYRROLE COMPOSITE SYSTEMS

Rajshekar.L.Madival[1], Vinay.V.Kannur[1], N.Nagaraja[1], Prashantkumar.M[2*]

Abstract

The Polypyrrole polymer composites containing ZnO nanoparticles (NPs) and Li_2O have been investigated for structural properties. The compositions of the type PPy50 + Li_2Ox + ZnO(50-x) NPs where x = 0, 2, 4, 6, 8, and 10, were prepared by employing ball milling method. Scanning Electron Microscope (SEM) and X-ray Diffraction (XRD) techniques were used to characterize the structural properties of as prepared samples. The spherical cluster of ZnO nanoparticle crystallites are shown in the SEM patterns as being surrounded by amorphous PPy/ZnoNps-Li_2O structures. XRD results revealed that both amorphous and Nano crystallite structures were present in the samples. Changes in the structural characteristics as well as the creation of complex nanocomposite clusters encircled by amorphous structures have been reported.

Keywords: Polypyrrole, Composites, XRD, SEM.

[1]Department of Physics Rao Bahadur Y Mahabaleswarappa Engineering College, Ballari, Karnataka, India
[2*]Department of PG Studies and Research in Physics Government College (Autonomous), Kalaburagi, Karnataka , India

***Corresponding Author:** Prashantkumar.M
*Department of PG Studies and Research in Physics Government College (Autonomous), Kalaburagi, Karnataka, India, Email: pacificmg@gmail.com

DOI: - 10.31838/ecb/2023.12.si5.088

1. INTRODUCTION

Semiconducting polymers are attractive to scientists and engineers in a range of disciplines due to their potential applications as electrodes (for electrochemical batteries and capacitors), energy storage devices, electro catalysts and sensors, anticorrosive coatings, etc. [1-2]. Generally speaking, polymers are thought to be non-conducting. Double-bonded conjugated polymers have semiconducting characteristics. With the right dopants, polypyrrole exhibits semiconducting characteristics [3]. The application and typical representative of conducting polymers point to the characteristics of the class of materials [4]. Numerous studies have shown that selective metal oxide doping can quickly improve the conductivity of poly-conjugated polymers with conductivities between 10^{-10} S/m and 10^{-5} S/m [5, 6–8]. Researchers have recently concentrated on improving the fabricability and other PPy features [9–11].

The composite material's conducting charac-teristics are improved by nanofillers in conducting polymers [12]. In PPy and other polymers,the ZnO nanoparticles (NPs) function as reinforce fillers [13–14]. Numerous researchers have noted recently that ZnO NPs have a large specific surface area, are non-toxic, inexpensive, and operate as an adsorbent[15–18]. Because of its size-dependent electrical and optical chara-cteristics, ZnO NPs have received a lot of attention as a semiconductor in recent years [19]. ZnO NPs are discovered to be easily produced in metals and have numerous uses in the electronic and medical fields [20]. The nanocomposite consists of metal and organic parts; the second part being responsible for enhancing the host materials' electrical properties while the first part attributes to increasing their mechanical qualities [21]. High UV absorption, a long lifespan [22], and a large volume ratio are all positive characteristics of ZnO NPs that make them suitable for use in gas sensors [23–24]. There are several ways to synthesise ZnO NPS [25–27]. Due to its high ionic conductivity and superionic conductivity, lithium oxide (Li_2O) has recently been used in energy storage devices for the next generation of electric vehicles [29], as well as in heart pacemakers, mobile phones, laptop computers, and lightweight, high power density solid state batteries. The polymer's molecular chains may attach during the in-situ polymerization process used to create PPy and act as filler [30–31].

ZnO NPs and lithium oxide are typically employed as dopants; the first is used to decorate PPy amorphous structures, and the second is used to implant ZnO NP crystallite clusters.

The mechanical mixing process is appropriate for large-scale manufacturing, and the type of synthesis provides beneficial electrical, chemical, and mechanical features for industrial production [32, 33], as well as their use in sensors and lithium-ion batteries [34, 35].

In the present work, the ZnO NPs and bulk Li_2O doped polypyrrole nanocomposites in the composition range, PPy_{50} + Li_2o_x + ZnO $_{(50-x)}$ NPs with x = 0, 2,4,6,8, and 10, labeled as PZL0, PZL2, PZL4, PZL6, PZL8 and PZL10 were synthesized and their structural properties have been investigated.

The objective of the present work is to understand the effect of incorporation of ZnO NPs and bulk Li_2O into pristine PPy over a wide range of composition. These composite systems have not been reported elsewhere, for their structural properties.

2. EXPERIMENTAL

The oxidizing agent Ammonium Persulphate (APS), Acetone, Li_2O, and Zinc Oxide Nanoparticles in powdered form (particle size being less than 100 nm) were the AR grade chemicals that were purchased from Sigma Aldrich. Pyrrole, a doubly distilled monomer, is in situ polymerized in the presence of ammonium persulphate in a beaker with a 0.3 M concentration (APS). A magnetic stirrer is used to hold the beaker. 0.6 M ammonium persulphate is added to 100ml of water. APS is gradually incorporated into 0.3 M Polypyrrole. The magnetic needle revolved constantly throughout the reaction's six-hour runtime at a temperature of 273 K to 278 K. The precipitate that resulted was removed using a filtration suction process, rinsed with deionized water, and dried in a hot air oven for six hours. The byproduct was burned to a temperature of 373 K in a muffle furnace, producing 2.25 g of the black Polypyrrole powder, which was then regarded as 100%.

A mechanical vibration mill (Make: Techno search instrument Mumbai, India) was used to grind the required weight % of PPy50, ZnO(50-x) NPs, and Li_2O(x). The mill was run for 15-20 minutes to produce a homogeneous combination of powder. The other samples were created using the same methodology, but with different compositions of x = 0, 2, 4, 6, 8 and 10 mole fraction weight percentage [36]. The labels for all of the samples

were PZL0, PZL2, PZL4, PZL6, PZL8, and PZL10.

3. RESULTS AND DISCUSSIONS

3.1 SEM Analysis

Figures (1a) to (1g) show the SEM images of PPy/ZnONps-Li_2O ternary composites for various weight percentages of PZL0, PZL2, PZL4, PZL6, PZL8, PZL10, and PPy. The SEM pictures of pure Polypyrrole (PPy) in Figure indicate a cluster of spherically shaped particles with the hallmarks of an amorphous nature (1g). The ZnO NPs were embedded in PPy and had loosely organized, approximately spherical grains, which allowed for the observation of the morphological alterations. Li_2O is introduced, resulting in the granular morphology depicted in Figures 1b to 1d. As seen in Figure 1e, the surface morphology of Li_2O in PZL8 has somewhat transformed into an agglomerated structure, and in PZL10, the agglomeration has increased. It is also observed that poly-pyrrole lithium decorated (PPy/ZnONps-Li_2O) amorphous structure Agglomeration of ZnO nanoparticles with different sizes.

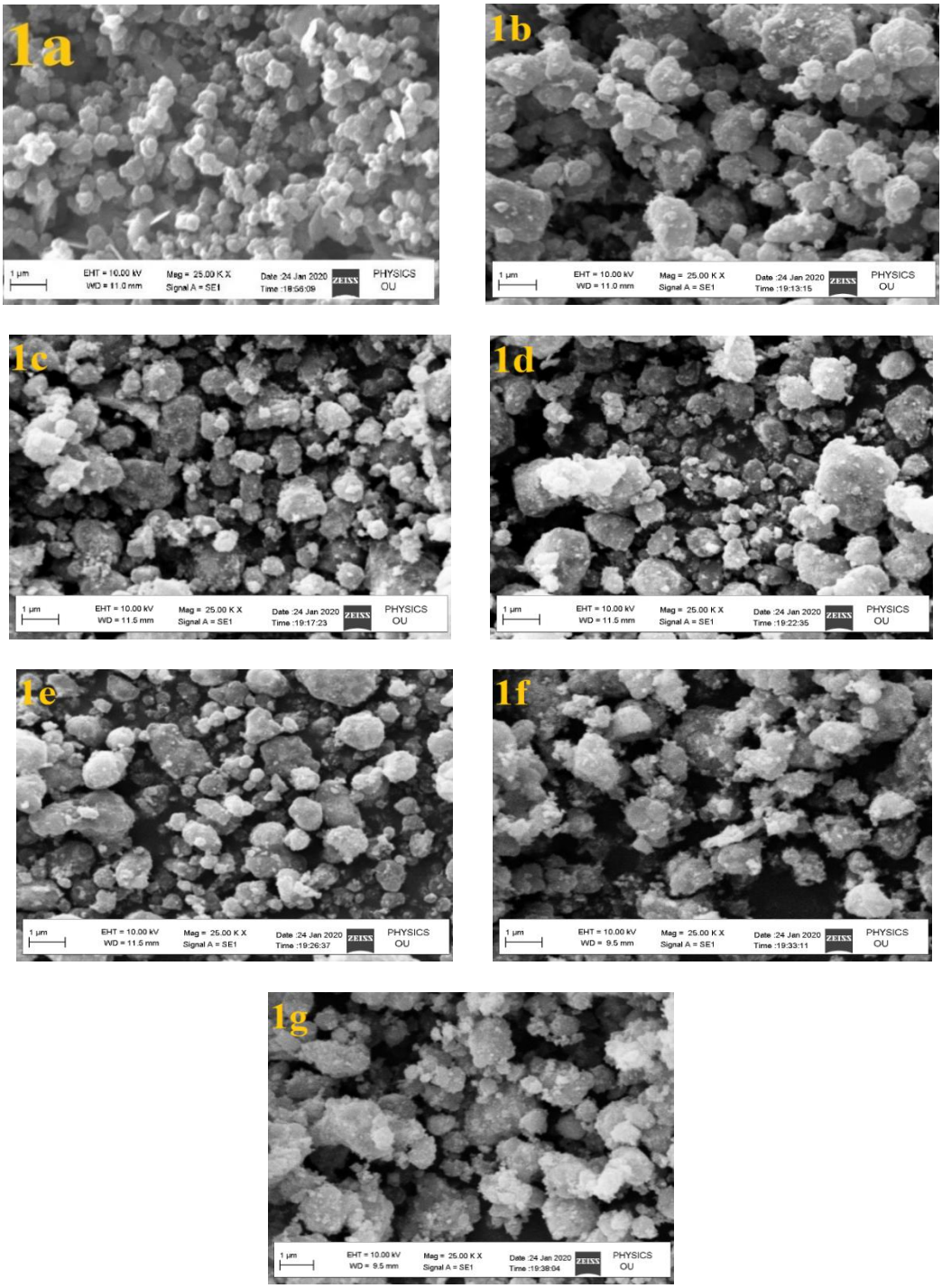

Fig 1. SEM images of Fig (1a) Pure PPy, (1b) PZL0, (1c) PZL2, (1d) PZL4, (1e) PZL6, (1f) PZL8 and (1g) PZL10.

3.2 *X-Ray Diffraction Analysis*

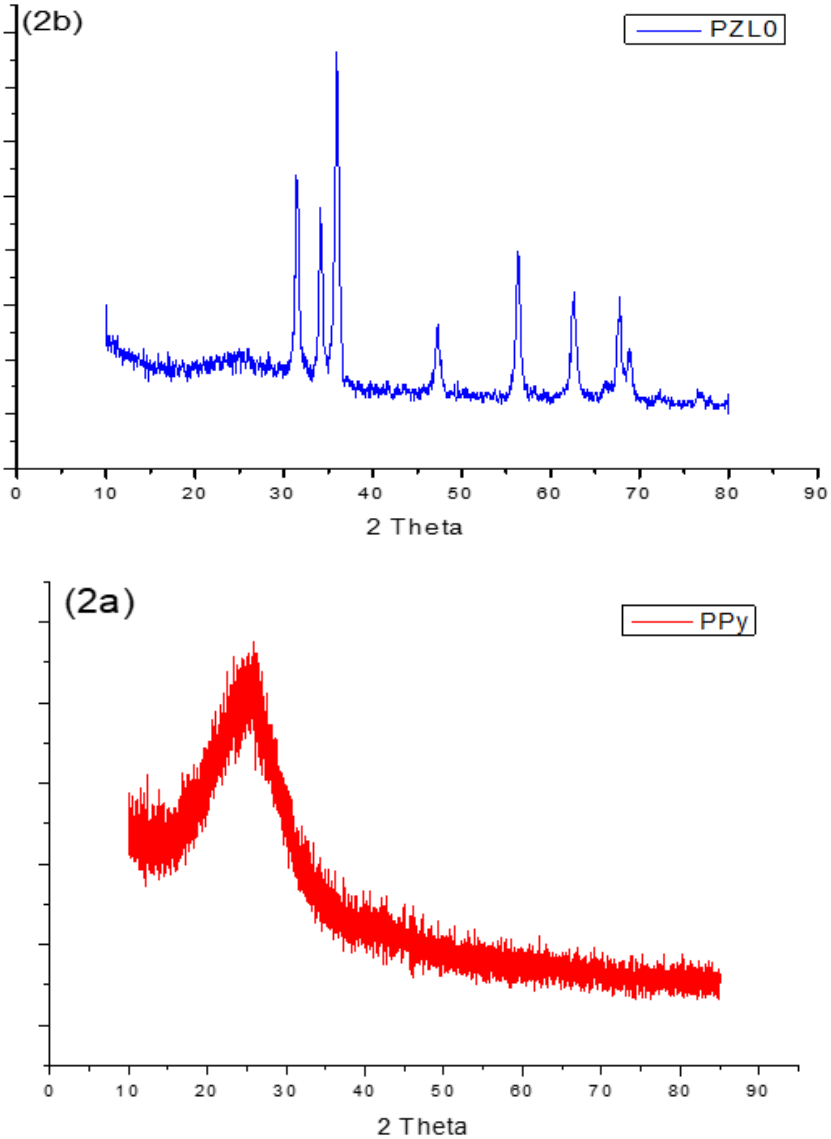

Fig. 2. X-ray Diffraction (a) PPy and(b) PZL0

XRD Williamson-Hall (W-H) analysis is a streamlined integral breadth approach used to calculate peak width-based estimates of crystallite size and lattice strain [37].

The amorphous structure of PPy was seen in the X-ray diffraction pattern displayed in fig. 2(a), with a peak value at 2θ =25.54°.

The PZL0 (PPy+ZnONPs 50 wt%) distinctive peak seen in figure 2 (b). There are 10 peaks that are present at 2=31.51°, 34.17 °, 36.00 °, 47.29 °, 56.35 °, 67.80 °, 68.76 °, 72.19 °, and 76.79 °; these peaks are assigned to the respective planes (100), (002), (101), (102), (110), (103), (200), (112), (201), (004), and 2θ X-ray diffraction measurements and the published JCPDS file no. (00-36-1451) are in good accord [38]. The nanoparticles' crystalline structure was clearly seen in the peaks of the XRD spectrum. The lattice constants a = 4.886 and C = 5.284 were obtained using the XRD peak positions; using these values, the ratio c/a=1.085A° has been calculated using the following relation [38].

$$\frac{1}{d_{hkl}} = \frac{4}{3}\left[\frac{h^2+k^2+hk}{a^2}\right] + \frac{l^2}{c^2} \qquad (1)$$

Where d hkl is the interplaner distance and (hkl) are the Miller indices of the specific plane in the XRD pattern, a and c are base vectors and constants. Equation (1)'s computed lattice constant is supported by the JCPDS file no. (00-36-1451), which is listed in table 1.

Table1. The 2θ, FWHM and d-spacing values of PZL0

[2θ]	FWHM	d-spacing [Å]
31.5118	0.3936	2.83913
34.1777	0.3936	2.62353
36.0073	0.4723	2.49431
47.2902	0.3936	1.9222
56.3585	0.3936	1.63254
62.5438	0.4723	1.48514
67.8047	0.551	1.38215
68.7643	0.4723	1.36519
72.1937	0.9446	1.30855
76.7992	0.96	1.24013

PPy/ZnO-Li_2O Composites PZL2, PZL4, PZL6, PZL8, and PZL10 displayed features peaks at 2θ= 29.84°, 31.53°, 34.17°, 36.02°, 47.31°, 56.36°, 62.64°, 67.66°, 68.77°, and 76.77° in Figure 2(b). The peaks were in good agreement with the JCPDS file number and nearly identical to the X-ray diffraction data of ZnO NPs (00-36-1451). Because the Li_2O adorned PPy is deposited on ZnO NPs, the peaks of Li_2O were adsorbed and held by ZnO Nps. In XRD patterns with Plane (101), a second peak at 2θ= 29.84° was seen. This peak is the typical peak of the defect that causes the augmentation of conductivity [39].

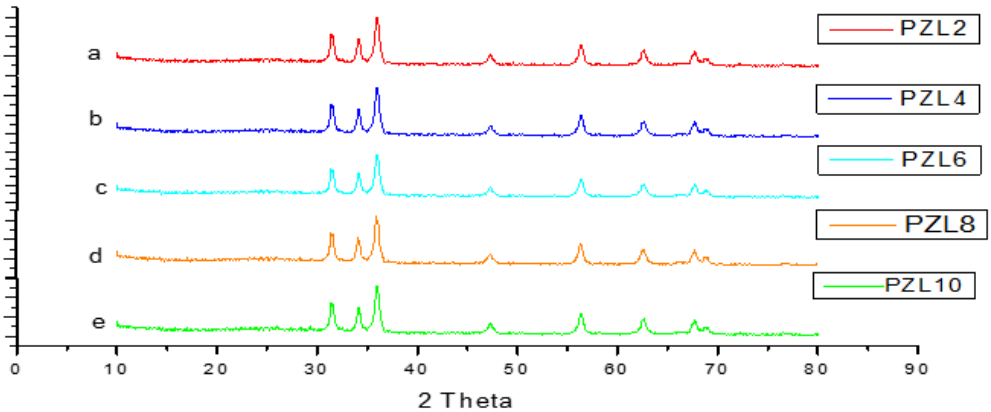

Fig2(b). X-ray Diffraction (XRD) PPy/ZnoNPs-Li_2o Composites (a) PZL2 (b) PZL4 (c) PZL6 (d) PZL8 (e) PZL10

Table2. The 2θ, FWHM and spacing valves of PZL10

[2θ]	FWHM	d-spacing [Å]
29.8419	0.4723	2.99409
31.5363	0.4723	2.83698
34.1722	0.3936	2.62394
36.0201	0.4723	2.49346
47.311	0.4723	1.9214
56.368	0.4723	1.63229
62.643	0.4723	1.48303
66.3097	0.551	1.40964
67.6649	0.6298	1.38467
68.7728	0.551	1.36504
76.7763	0.96	1.24045

The table 2 shows the 2θ, FWHM and interplaner spacing values of PZL10. In the XRD pattern, the (100) plane's greatest peak intensity was seen. When utilizing the Debye-Scherrer formula, which is provided below [40], this value is taken into account to get the average particle size of PZL0.

$$b = \frac{k\lambda}{\beta cos\theta} \qquad (2)$$

where d is grain size and β is the full width half maxima (FWHM) of the particular peak, k is the Scherer constant and is given by the value 0.9, θ is the Bragg's angle , λ= 1.5418Aº is the wavelength of CuKα source radiation [40] .

Using equation (2), it was determined that the ZnO nanoparticles in the material composite had an average size of about 20.26 nm. Table 1 contains the experimentally observed FWHM and interplaner spacing data for the Composite PZL0.

Dislocation density is the length of dislocation lines per unit volume of the crystal was determined by the following equation [40] .

$$\delta = \frac{1}{b^2} \qquad (3)$$

Where d is the crystalline size. The dislocation density value for PZL0 from the data of XRD was calculated and is equal to 2.2710^{-3} $(nm)^{-2}$

CONCLUSION

The Polypyrrole/ZnO NPs-Li_2O ternary composites were created, and they were then analysed using SEM and XRD methods. The SEM revealed that the particle agglomeration increased in the 10% weight percentage compared to other weight percentages. PZL0 (PPy/ZnONPs 50wt%) exhibits mirage features with Pure ZnO NPS in the XRD pattern, but PZL10 (PPy/ZnONPS-Li_2o 10wt%) has an extra peak.

REFERENCES

1. N.Z.I.Bohari,Z.A.Talib,M.Amirul,S.M.Yunos, A.Kassim,Int.J.Phys,Sci.7,10,1670(2012).
2. S.E. Gamal, A.M. Ismail, R.E. Mallawany, Dielectric and nano- scale free volume properties of polyaniline/polyvinyl alcohol nanocomposites. J. Mater. Sci. 26, 7544–7553 (2015).
3. K. Suhailath, M.T. Ramesan, Temperature dependent AC conduc- tivity, mechanical and different DC conductivity modeling of poly (butyl methacrylate)/samarium doped titanium dioxide nanocom- posites. Journal of Materials Science: Materials in Electronics September 2017 ,28(18):13797-13805.
4. Gunnar F. Nordberg, Bruce A. Flower and Monica Nordberg Handbook on the Toxicology of Metals, Fourth Edition 2014.
5. Ratkovich A, Penn RL, Zinc oxide nanoparticle growth from homogenous solution: influence of Zn:OH, water concentration and surfactant additives. Mater. Res. Bull. 44(5):993–998 (2009).
6. Akhoon SA, Rubab S, Shah MA, A benign hydrothermal synthesis of nanopencils-like zinc oxide nanoflowers. Int Nano Lett 5:9–13 (2015).
7. Yu DH, Cai RX, Liu ZH, Studies on the photodegradation of rhodamine dyes on nanometer-sized zinc oxide. Spectrochim Acta A 60:1617–1624 (2004).
8. Curridal ML, Comparelli R, Cozzli PD, Mascolo G, Agostiano A, Colloidal oxide nanoparticles for the photocatalytic degra- dation of organic dye. Mater Sci Eng C Biomim Mater Sens Syst 23:285–289 (2003).
9. Chu SY, Yan TM, Chen SL, Characteristics of sol–gel syn- thesis of ZnO-based powders. J Mater Sci Lett 19:349–352 (2000).
10. Damonte LC, Mendoza-Zélis LA, Soucase BM, Hernández- Fenollosa MA, Nanoparticles of ZnO obtained by mechan- ical milling. Powder Technol 148:15–19 (2004).
11. Dai ZR, Pan ZW, Wang ZL, Novel nanostructures of functional oxides synthesized by thermal evaporation. Adv Funct Mater 13:9–24(2003).
12. T V Vernitskaya, O N Efimov, Russian Chemical Reviews 66 (5) 443 - 457 (1997).
13. M Aldissi (Ed.) Intrinsically Conducting Polymers: An Emerging Technology (Dordrecht: Kluwer Academic,) (1993).
14. M. H. Harun, E. Saion, A. Kassim, N. Yahya, andE. Mahmud, J. Acoust. Soc. Am. 2, 63 (2007).
15. G. Inzelt, J. Solid State Electrochem. 15, 1711 (2011).
16. J. L. Bredas and G. B. Street, Acc. Chem. Res. 18, 309 (1985).
17. Q. Cheng, Y. He, V. Pavlinek, C. Li, P. Saha, Surfactant-assisted polypyrrole/titanate composite nanofibers: morphology, structure and electrical properties. Synth. Met. 158, 953–957 (2008).
18. H. Behniafar, K. Malekshahinezhad, A unique path to reach thermo-stable polypyrrole/Pd microfibers via chemical oxidative polymerization. Colloid Polym. Sci. 292, 2083–2088 (2014).
19. D.S. Lee, D.D. Lee, H.R. Hwang, J.H. Paik, J.S. Huh, J.O. Lim,J.J. Lee, Characteristics of electrochromic device with polypyrrole and WO3. J. Mater. Sci. 12, 41–44 (2001).
20. M.T. Ramesan, V. Nidhisha, P. Jayakrishnan, Facile synthesis, characterization and material properties of novel poly (vinyl cin- namate)/nickel oxide nanocomposites. Polym. Int. 66, 548–556 (2017).
21. X. Ma, A. Liu, H. Xu, G. Li, Growth of ramification like ZnO rods in the presence of polyaniline. Colloid Polym. Sci. 285, 1631–1635 (2007).

22. J. Huang, Y. Yang, Synthesis of ZnO/polypyrrole composites and an application in Zn/Ni rechargeable batteries. RSC Adv. 4, 19205–19209 (2014).
23. Nguyen-Le, M.T.; Lee, B.K.: High temperature synthesis of inter- facial functionalized carboxylate mesoporous TiO2 for effective adsorption of cationic dyes. Chem. Eng. J. 281, 20–33 (2015).
24. Tajizadegan, H.; Torabi, O.; Heidary, A.; Golabgir, M.H.; Jamshidi, A.: Study of methyl orange adsorption properties on ZnO–Al2O3 nanocomposite adsorbent particles. Desalin. Water Treat. 57, 12324–12334 (2016).
25. Salem, A.N.M.; Ahmed, M.A.; El-Shahat, M.F.: Selective adsorp- tion of amaranth dye on Fe3O4/MgO nanoparticles. J. Mol. Liq. 219, 780–788 (2016).
26. Nassar, M.Y.; Mohamed, T.Y.; Ahmed, I.S.; Samir, I.: MgO nanos- tructure via a sol–gel combustion synthesis method using different fuels: an efficient nano-adsorbent for the removal of some anionic textile dyes. J. Mol. Liq. 225, 730–740 (2017).
27. Prabhatasree Goel, N. Choudhury, and S. L. Chaplot Superionic behavior of lithium oxide Li2O, PHYSICAL REVIEW B 70, 174307 (2004).
28. D. A. Keen, J. Phys.: Condens. Matter 14, R819 (2002).
29. M. Faisal, and S. Khasim, Polym. Sci., Ser. A, 56, 366 (2014).
30. D.G. Papageorgiou, I.A. Kinloch, and R.J. Young, Carbon,95, 460 (2015).
31. M. Dhingra, S. Shrivastava, P.S. Kumar, and S. Annapoorni, Compos. Part B, 45, 1515 (2013).
32. J. Huang, T. Yang, Y. Kang, Y. Wang, and S. Wang, J. Nat. Gas Chem., 20, 515 (2011).
33. H. Zheng, N.M. Ncube, K. Raju, N.N. Mphahlele, and M. Mathe, Springerplus, 5, 630 (2016).
34. Suryanarayana, C., Norton, M.G.: X-ray diffraction: a practical approach. Plenum Press Publishing, New York (1998).
35. L. Gang, L. Xia, S. Xinghua, Y. Jian, and H. E. Jiasong, Front. Chem. Eng. China 2 (2), 118 (2007).
36. Yasin, S. F.; Zihlif, A. M.; Ragosta, A. J. The Electrical Behavior of Laminated Conductive Polymer Composite at Low Temperatures. J. Mater. Sci. 16, 63–69 (2005).
37. Basavaraja, C.; Won, J. K.; Thinh, P. X.; Do, S. H. Electrical Conductivity Studies on Water-Soluble PPy–Graphene Oxide Composites. Polym. Compos, 32, 2076–2083 (2011).
38. Jing, L.; Jang-Kyo, K. Percolation Threshold of Conducting Polymer Composites Containing 3D Randomly Distributed Graphite Nanoplatelets. Compos. Sci. Technol. 67, 2114–2120 (2007).
39. M.V.Murugendrappa, SyedKhasimand M.V.N.Ambika Prasad, Bull.Mater. Science28, 565-569 (2005).
40. B. Chetan, H.G.RajPrakash, Y.T.Ravikiran, S.C.Vijayakumari, CH.V.V.Ramana, S.Thomas, Daewon Kim, Enhancing humidity Sensing Performance of Polyaniline/water Soluable Graphene Oxide Composite. The international Journal of pure and Applied Chemistry, Talanta Volume 196, 1 May 2019, Pages 337-344.